JACS
JOURNAL OF THE AMERICAN CHEMICAL SOCIETY
Article
pubs.acs.org/JACS

# A QM/MM Study of the L-Threonine Formation Reaction of Threonine Synthase: Implications into the Mechanism of the Reaction Specificity

Mitsuo Shoji,*[,†,‡] Kyohei Hanaoka,[‡] Yuzuru Ujiie,[‡] Wataru Tanaka,[‡] Daiki Kondo,[‡] Hiroaki Umeda,[†] Yoshikazu Kamoshida,[§] Megumi Kayanuma,[∥] Katsumasa Kamiya,[†] Kenji Shiraishi,[†] Yasuhiro Machida,[⊥] Takeshi Murakawa,[#] and Hideyuki Hayashi[⊥]

[†]Center for Computational Sciences, University of Tsukuba, Tennodai 1-1-1, Tsukuba 305-8577, Japan
[‡]Graduate School of Pure and Applied Sciences, University of Tsukuba, Tennodai 1-1-1, Tsukuba 305-8571, Japan
[§]Information Technology Center, The University of Tokyo, Yayoi 2-11-16, Bunkyo-ku, Tokyo 113-8658, Japan
[∥]Graduate School of Systems and Information Engineering, University of Tsukuba, Tennodai 1-1-1, Tsukuba 305-8573, Japan
[⊥]Department of Chemistry, Osaka Medical College, Takatsuki 569-8686, Japan
[#]Department of Biochemistry, Osaka Medical College, Takatsuki 569-8686, Japan

Supporting Information

**ABSTRACT:** Threonine synthase catalyzes the most complex reaction among the pyridoxal-5′-phosphate (PLP)-dependent enzymes. The important step is the addition of a water molecule to the C$\beta$−C$\alpha$ double bond of the PLP−$\alpha$-aminocrotonate aldimine intermediate. Transaldimination of this intermediate with Lys61 as a side reaction to form $\alpha$-ketobutyrate competes with the normal addition reaction. We previously found that the phosphate ion released from the *O*-phospho-L-homoserine substrate plays a critical role in specifically promoting the normal reaction. In order to elucidate the detailed mechanism of this "product-assisted catalysis", we performed comparative QM/MM calculations with an exhaustive search for the lowest-energy-barrier reaction pathways starting from PLP−$\alpha$-aminocrotonate aldimine intermediate. Satisfactory agreements with the experiment were obtained for the free energy profile and the UV/vis spectra when the PLP pyridine N1 was unprotonated and the phosphate ion was monoprotonated. Contrary to an earlier proposal, the base that abstracts a proton from the attacking water was the $\varepsilon$-amino group of Lys61 rather than the phosphate ion. Nevertheless, the phosphate ion is important for stabilizing the transition state of the normal transaldimination to form L-threonine by making a hydrogen bond with the hydroxy group of the L-threonine moiety. The absence of this interaction may account for the higher energy barrier of the side reaction, and explains the mechanism of the reaction specificity afforded by the phosphate ion product. Additionally, a new mechanism, in which a proton temporarily resides at the phenolate O3′ of PLP, was proposed for the transaldimination process, a prerequisite step for the catalysis of all the PLP enzymes.

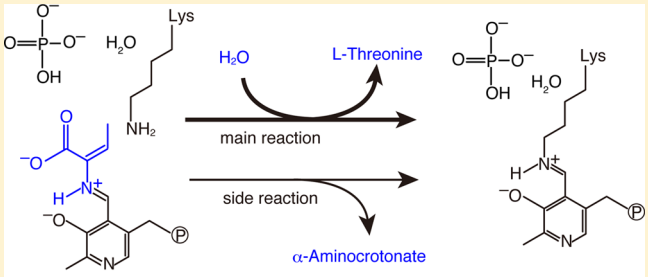

Reaction Mechanism of Threonine Synthase

## INTRODUCTION

Threonine synthase (ThrS) is a pyridoxal 5′-phosphate (PLP) dependent enzyme that catalyzes the formation of L-threonine from *O*-phospho-L-homoserine (OPHS). This is the final step of the threonine biosynthetic pathway, which exists in bacteria, yeast, and plants. As threonine is not synthesized in mammals, ThrS can be a target for novel antibiotics. The remarkable feature of ThrS is that the reaction is the most complicated among PLP enzymes; it involves all types of intermediates known to PLP enzymes. Accordingly, there are many opportunities of side reactions, but ThrS carries out regiospecific and stereospecific reactions and produces L-threonine with a high selectivity.[1−5] Therefore, knowledge about the ThrS reaction mechanism is of great importance both for fundamental enzymology and practical purposes.

A proposed reaction mechanism of ThrS starts with the PLP−Lys aldimine (**1**) and OPHS, involves seven intermediate states from the PLP−OPHS aldimine (**2**) to the PLP−L-threonine aldimine (**8**), and ends with the concomitant regeneration of **1** and the production of L-threonine (full reaction cycle is shown in Figure S1, Supporting Information).[2,5] In addition to catalyzing the normal reaction to form L-threonine, ThrS also catalyzes the formation of $\alpha$-ketobutyrate via $\alpha$-aminocrotonate as a side reaction (**6** → **1**). The

**Received:** August 24, 2013
**Published:** February 25, 2014

   dx.doi.org/10.1021/ja408780c | J. Am. Chem. Soc. 2014, 136, 4525−4533

intermediate state **6**, PLP−$\alpha$-aminocrotonate aldimine, is the branching point of the two pathways. In *Thermus thermophilus* HB8 ThrS (tThrS), the side reaction is suppressed to ∼1% of the total reaction; i.e., ∼99% of the flow from **5** is diverted to the **6** → **7** → **8** → **1** pathway. Therefore, there must be a mechanism that selectively accelerates the **6** → **7** → **8** → **1** pathway compared to that of the **6** → **1** pathway. Recently, we found that the phosphate ion released from the OPHS substrate at the **4** → **5** step remains at the active site and is crucial for lowering the energy barrier of the **6** → **7** → **8** → **1** pathway.[5] Thus, "product-assisted catalysis", which was first proposed for 8-oxoguanine DNA glycosylase,[6] was considered to operate in ThrS and is the basis of the reaction specificity. As a sulfate ion cannot substitute for the phosphate ion, it was suggested that the phosphate ion may act as a base catalyst, removing a proton from the water molecule attacking C$\beta$ at the step **6** → **7**. However, the precise mechanism of the catalysis by the phosphate ion is not clear at present. Especially, information on the protonation structures of the intermediates of ThrS, which strongly affects the catalytic properties of the coenzyme, is not fully obtained, although it is absolutely necessary for discussing the mechanism.

It is now well accepted that quantum chemical calculations provide important information about the reaction mechanism of enzymatic catalysis. However, evaluation of the validity of the calculation is often difficult, especially when there is not enough experimental data on the free energy profile. The elementary steps of **6** → **7** → **8** → **1** and **6** → **1** were analyzed in detail for tThrS by following the reaction of tThrS with L-threonine, and the free energy profiles for these steps have been obtained.[5] This allows us to compare the results of quantum chemical calculations with the experimental data. In this study, the complete reaction mechanism of tThrS for the steps after the branching point of **6**, i.e., the steps connecting intermediates **6**, **7**, **8**, and the Michaelis complexes with L-threonine ($\mathbf{1}^{\mathbf{Thr}}$) and $\alpha$-aminocrotonate ($\mathbf{1}^{\mathbf{AC}}$), was investigated by using a quantum mechanics/molecular mechanics (QM/MM) method. In order to validate the reaction mechanism, we extensively explored for models different in the protonation states of the PLP N1 and the phosphate ion and the reaction pathways such as the proton transfer route. In addition, other important aspects of the reaction pathway—replenishment of the reacting water molecule and open−closed conformational change—are presented to deepen the understanding of the ThrS mechanism.

## COMPUTATIONAL DETAILS

We performed the hybrid quantum mechanics/molecular mechanics (QM/MM) calculations using the NWChem program package.[7] The QM region included PLP, the phosphate ion, 3(4) waters, ((W−1), W0, W5, W6), as well as the key side chains of Lys61, Arg160, Ser84, Thr88, and Thr317 (approximately 100 atoms, see Figure 1 and Figure S2, Supporting Information). W−1 was included in the QM region for the steps $\mathbf{6}^{\mathbf{H_2O}}$ → **7** → **8** → **1**. The density functional theory (B3LYP/6-31G*) was used for QM, while the remaining atoms were subjected to an AMBER-99 force field. An electronic embedding scheme was adopted, and hydrogen link atoms were employed for the QM/MM boundary. The initial coordinates were taken from the X-ray structure of tThrS complexed with an analogue for the PLP−$\alpha$-aminocrotonate aldimine and a phosphate ion determined at a 2.1 Å resolution (PDB ID: 3AEX). After protonation and replacing the analogue in the original crystal structure with the PLP−$\alpha$-aminocrotonate aldimine of **6**, the system is solvated by a water droplet with a 45 Å radius, and an initial geometrical optimization was performed at the molecular mechanics level for the entire core, fixing the protein backbone atoms, PLP−$\alpha$ aminocrotonate aldimine, and phosphate ions without external potential. Force field parameters of nonstandard molecules, PLP and phosphate ion, were constructed by combining typical force field parameters. The total charges at the PLP N1 deprotonated model were −4$e$ and −4$e$ for the QM and whole system, respectively. QM/MM geometry optimizations were performed for all atoms within a 12 Å radius of a fixed QM center (approximately 800 atoms). No cutoff for the nonbonded interactions was used for the QM−MM interactions.

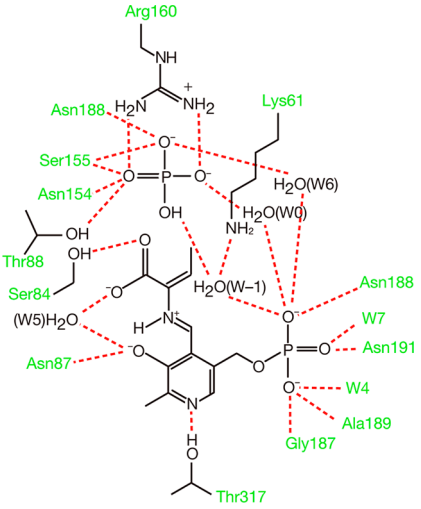


**Figure 1.** Arrangement of the tThrS active site at the PLP−$\alpha$-aminocrotonate aldimine intermediate ($\mathbf{6}^{\mathbf{H_2O}}$). The QM and MM regions are colored black and green, respectively. The hydrogen bonds are denoted by the dashed red lines. The numbering of water molecules, W5 and W6, is as in ref 4. Two water molecules, W−1 and W0, are newly introduced. W−1 is supplied by migration of W0, the latter of which is then replenished from a solvent water to form $\mathbf{6}^{\mathbf{H_2O}}$. Accordingly, $\mathbf{6}^{\mathbf{H_2O}}$ contains W−1 but **6** does not contain W−1.

The hydrogen-bond networks and orientations of the phosphate ion and water molecules were searched for all the possibilities by performing QM/MM optimization calculations. For the position and orientation of W0 and W−1 in **6** and $\mathbf{6}^{\mathbf{H_2O}}$, we obtained the energetically most stable positions and orientations. These water molecules fit in the hydrogen bond network with surrounding water molecules and polar groups. However, W−1 has a metastable state different from the most stable state. From this state, the reaction proceeded through a path that has a higher energy barrier than the energetically favorable path. This is described in the Supporting Information (The Metastable State of W−1). The phosphate ion is strongly held by Arg160 through a strong bidentate bridge. We checked the location of the phosphate ion by changing the bidentate fashion to monodentate, or rotating 90° around the C$\zeta$:Arg160−P axis, but these alterations all caused destabilization. The positions of the side chain atoms of Lys61 in **6** and $\mathbf{6}^{\mathbf{H_2O}}$ are essentially the same as those of the crystal structure (3AEX), except for the $\varepsilon$-amino group of $\mathbf{6}^{\mathbf{H_2O}}$, which is slightly shifted toward W−1 along the hydrogen bond. We also checked the validity by performing another set of classical molecular dyanamics simulations (unpublished). The reaction pathways were searched using the nudged elastic band (NEB) algorithm, and the transition states were refined from the NEB transition states by searching for the first-order saddle points. The free energies were evaluated by carrying out the normal-mode analysis in the QM region. TD-DFT calculations were performed for the UV/vis absorption spectra at the CAM-B3LYP/6-311+G* level.[8]

## RESULTS AND DISCUSSION

**Reaction Mechanism.** The most favorable reaction mechanism and the free energy profile are shown in Figures


dx.doi.org/10.1021/ja408780c | J. Am. Chem. Soc. 2014, 136, 4525−4533

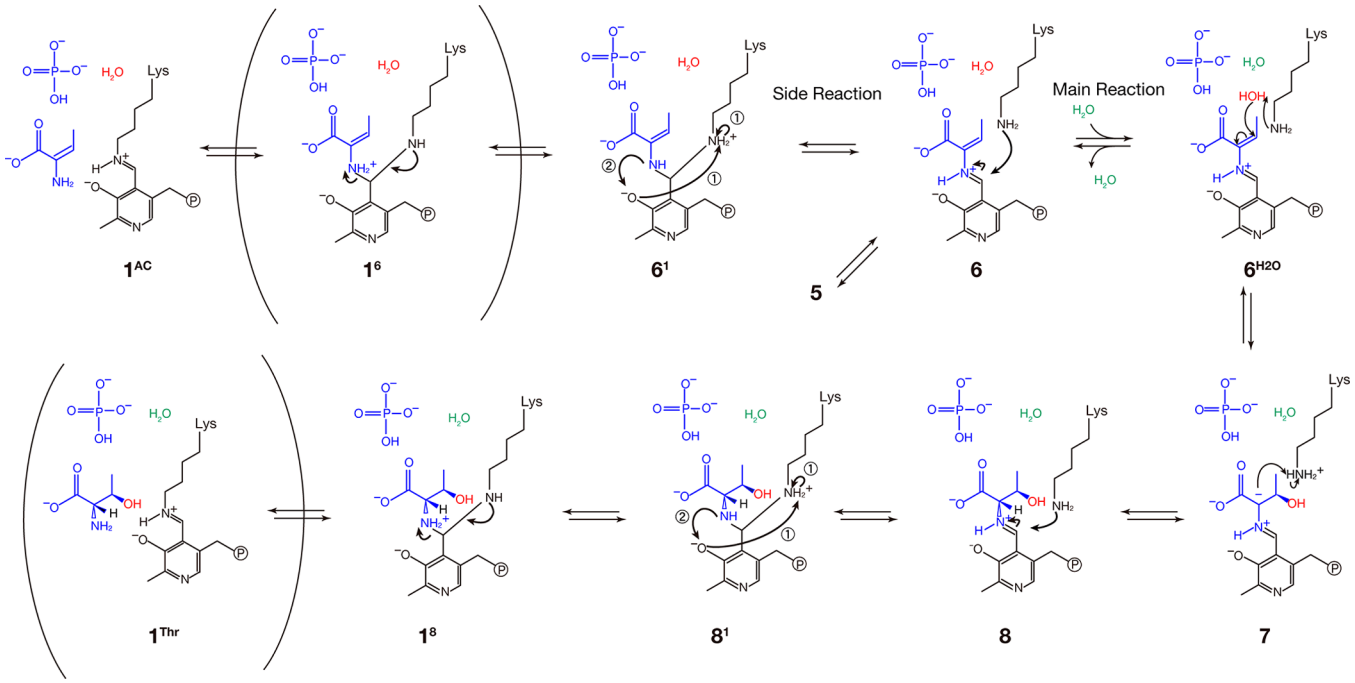


**Figure 2.** Calculated mechanism of tThrS from the aldimine intermediate (**6**) to L-threonine ($\mathbf{1}^{Thr}$) and to $\alpha$-aminocrotonate ($\mathbf{1}^{AC}$), which are the main and side reaction pathways, respectively. $\mathbf{1}^{AC}$ and $\mathbf{1}^{Thr}$ are the internal aldimine states with bound products (Michaelis complexes). The important hidden states ($\mathbf{1}^{6}$ and $\mathbf{1}^{Thr}$), which exist on the reaction pathway but were not obtained as stationary points in our theoretical calculations, are shown in parentheses. Substrate/product moiety and the phosphate ion are colored blue and key water molecules are colored red for easy identification.

2 and 3, respectively. (Free energy contributions are summarized in Table S1 (Supporting Information). A full NEB reaction profile is shown in Figure S3, Supporting Information.) These results are obtained after extensive searches for the (i) protonation state of PLP N1, (ii) protonation state of the phosphate ion, (iii) state of the water molecules, and (iv) arrangement of hydrogen bonds, during the reaction by performing geometry optimization for each state. In the case of the (i) unprotonated PLP N1, (ii) monoprotonated phosphate ion, (iii) presence of a water molecule for the nucleophilic attack at C$\beta$, and (iv) hydrogen bond formation between Ser155 and the phosphate ion, the free energy profile is qualitatively in good agreement with the experimental result within ±3 kcal mol$^{-1}$. The optimized structures for all the intermediates and transition states are shown in Figure 4. Enlarged views are shown in Figure S4 (Supporting Information).

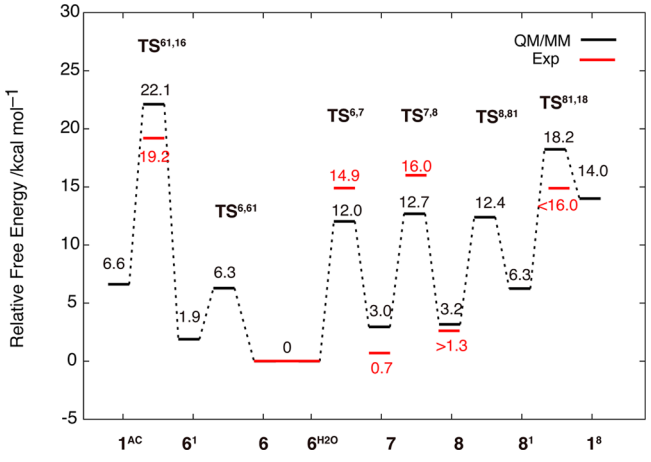


**Figure 3.** Calculated free energy profile of tThrS at the QM/MM level. The relative energies are given with respect to the aldimine intermediates (**6** and $\mathbf{6}^{H_2O}$). The energy levels of 6 and $6^{H_2O}$ are set to be equal to each other (see text for discussion).

We performed additional QM/MM calculations to investigate the dependencies on (1) counterion, (2) basis sets, and (3) van der Waals (vdw) correction in the QM/MM treatment (calculated relative energies are summarized in Table S2, Supporting Information). For (1), 4 $Na^+$ ions are placed on the outer surface of the water droplet according to the electrostatic potential. The $Na^+$ ions are away from the center of the system (center of the two N atoms of PLPs) by 43−50 Å, which is reasonable compared to our 100 ns molecular dynamics (MD) results (details of the MD results will be described elsewhere). The energy changes by the counterions were within 0.3 kcal mol$^{-1}$, indicating that the direct effect from the counterions in solvent is negligibly small. For (2), single point calculations with 6-311G** basis sets were performed for all states in the energy profile. The energy difference was largest for $1^8$ but was an increase by only 3.4 kcal mol$^{-1}$. For (3), Grimme's dispersion correction was used.[9] Compared to the energies at the same basis set level of 6-311G**, the contributions from the vdw interactions were within 2 kcal mol$^{-1}$. States $\mathbf{7}-\mathbf{TS}^{8,81}$ were more stabilized and states $\mathbf{8}^{1}-\mathbf{1}^{8}$ were more destabilized. The total contributions from the basis set and the vdw interactions are within 2.3 kcal mol$^{-1}$ in states $\mathbf{1}^{AC}-\mathbf{TS}^{8,81}$ and within 5.3 kcal mol$^{-1}$ in states $\mathbf{8}^{1}-\mathbf{1}^{8}$. It is noted that a relatively large energy shift is in the transaldimination step, $\mathbf{8}^{1}-\mathbf{1}^{8}$. As discussed in the "Open−Closed Conformational Change" section, after the transaldimination process, a large open−closed conformational change, which is not handled in the current QM/MM calculations, may stabilize the state of $\mathbf{1}^{Thr}$


dx.doi.org/10.1021/ja408780c | J. Am. Chem. Soc. 2014, 136, 4525−4533

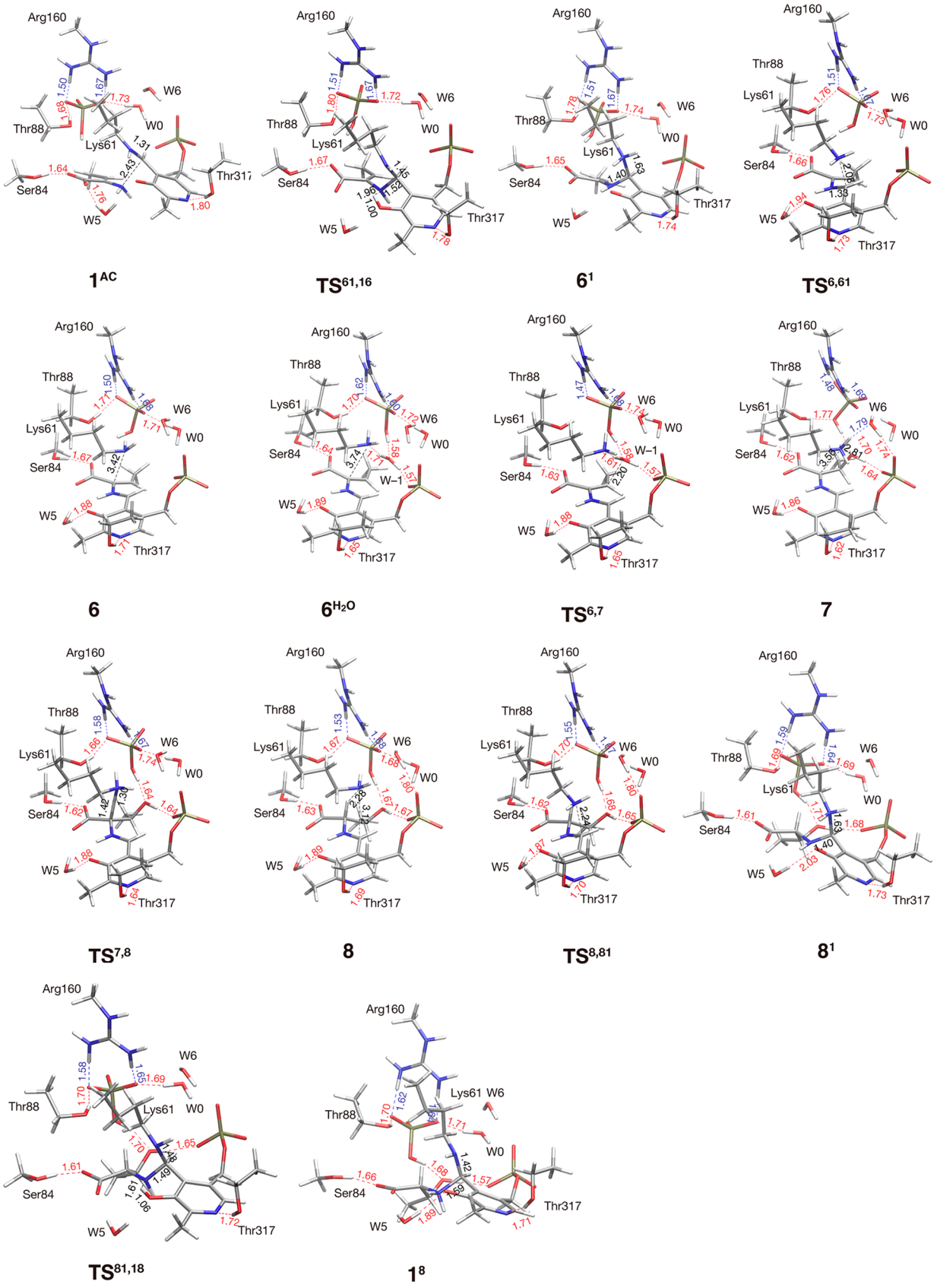


**Figure 4.** QM/MM optimized structures of the intermediates and transition states. The hydrogen bonds and important distances are denoted by colors and black, respectively. Only the QM atoms are shown for clarity. Enlarged views are shown in Figure S4 (Supporting Information).

and affect the states $8^1$–$1^8$. The energy level of $TS^{81,18}$ is still lower than that of $TS^{61,16}$ even after the recalculation described above. Thus, the total energy contributions from (1) counterion, (2) basis set, and (3) vdw interactions are not


dx.doi.org/10.1021/ja408780c | J. Am. Chem. Soc. 2014, 136, 4525–4533

large compared to other reaction pathways and other factors such as the PLP N1 protonation state and the existence of water molecule as discussed in later sections.

The calculated reaction mechanism is comprised of two types of reaction steps: (1) the water addition steps in the normal reaction and (2) the transaldimination steps in both the normal and side reactions. In the next three sections, these two types of reaction steps in ThrS as revealed by the QM/MM calculations are described in detail, together with the consistency of our intermediate models with the UV/vis spectra. In the subsequent two sections, the possibilities of other protonation states and reaction pathways are examined to validate the reaction mechanism. Later, considerations on other important aspects of the reaction pathway—replenishment of the reacting water molecule and open−closed conformational change—are presented. Finally, on the basis of these findings, the role of the product phosphate ion, which is absolutely required for ThrS to carry out a specific catalysis, is discussed.

**Addition of a Water Molecule to Cβ−Cα.** In the aldimine intermediates of **6** and $\mathbf{6}^{\mathbf{H_2O}}$, where $\mathbf{6}^{\mathbf{H_2O}}$ contains one additional water molecule (W−1) for the addition reaction, the ε-amino group of Lys61 is in the unprotonated form ($-NH_2$). W−1 is excluded from the solvent, while W0 and W6 are almost exposed to the solvent. Therefore, we consider that W−1 is provided by the migration of W0, and W0 is replenished from the bulk solvent to form $\mathbf{6}^{\mathbf{H_2O}}$. W0 and W6 make hydrogen bonds with the O atoms of the phosphate ion and the PLP phosphate group. The reacting water, W−1, is close to PLP Cβ (Cβ−O:W−1 distance is 2.44 Å) and is stabilized by the three hydrogen bonds with N of the Lys61 ε-amino group, H of the phosphate ion, and O of the PLP phosphate group. The nucleophilic attack of this water molecule on Cβ forms a quinonoid intermediate (**7**). The transition state ($\mathbf{TS}^{6,7}$) is found at a Cβ−O:W−1 distance of 2.20 Å. After $\mathbf{TS}^{6,7}$, a proton is transferred from the reacting water to the Lys61 ε-amino group to form a protonated ε-amino group ($-NH_3^+$). The calculated free energy barrier for $\mathbf{TS}^{6,7}$ is 12.0 kcal mol$^{-1}$ which can be favorably compared to the experimental value of 14.9 kcal mol$^{-1}$.[5] Most importantly, the base that abstracts the proton from the attacking water is the ε-amino group of Lys61, not the phosphate ion as previously suggested.[5] The N:Lys61−H:W−1 distance decreases from 1.71 Å in **6** to 1.61 Å in $\mathbf{TS}^{6,7}$, indicating that the ε-amino group of Lys61 stabilizes $\mathbf{TS}^{6,7}$. In $\mathbf{TS}^{6,7}$, the monohydrogen phosphate ion makes a hydrogen bond with the reacting water molecule. However, the H:phosphate−O:W−1 distance is unchanged from that of **6**, suggesting that the phosphate ion may not significantly contribute to the stabilization of $\mathbf{TS}^{6,7}$. Mulliken bond orders for Cβ−O:W−1 are 0.05, 0.12, and 0.82 for **6**, $\mathbf{TS}^{6,7}$, and **7**, respectively (Table S3, Supporting Information), indicating that $\mathbf{TS}^{6,7}$ is an early transition state in the Cβ−O bond formation. This is also reflected in the full energy profile (Figure S3, Supporting Information).

Another structural feature of **7** is the strong hydrogen bond between PLP N1 and Thr317 O, with the distance of 1.62 Å between N1 and the hydroxy H being the shortest among all the calculated states. Calculated atomic charges showed an increase of the negative charge at Cα, C4′, and N1 by 0.06*e* (0.06*e*), 0.19*e* (0.19*e*), and 0.03*e* (0.04*e*), respectively, in **7** compared to $\mathbf{6}^{\mathbf{H_2O}}$ at the Mulliken (Lowdin) population analysis (Tables S4 and S5, Supporting Information). These charge distribution changes clearly show the large delocalization of the negative charge at Cα, developed after the nucleophilic attack at Cβ to the PLP moiety in **7**. This, on the other hand, indicates that the hydrogen bond contributes to the stabilization of **7**, which in many PLP enzymes other than the fold type II is brought about by protonation at PLP N1.

The next step is a proton transfer from the ε-amino group of Lys61 to Cα. The transition state ($\mathbf{TS}^{7,8}$) is characterized by the distances N:Lys61−H = 1.30 Å and H−Cα = 1.42 Å; these distances are (1.04 Å, 2.98 Å) and (2.28 Å, 1.09 Å) for **7** and **8**, respectively. The calculated relative free energy of $\mathbf{TS}^{7,8}$ is 12.7 kcal mol$^{-1}$, which is also comparable to the experimental value of 16.0 kcal mol$^{-1}$.[5] Interestingly, the ε-amino group of Lys61 does not significantly move closer to Cα, because Cα gets closer to the ε-amino group by changing the hybridization type from $sp^2$ to $sp^3$. In this transformation, Mulliken atomic charge at Cα is 0.23*e*, −0.14*e*, and −0.05*e* for **7**, $\mathbf{TS}^{7,8}$, and **8**, respectively, also indicating the hybridization conversion and the resultant breaking of the π-conjugation of Cα with the neighboring protonated imino group.

The α-aminocrotonate moiety of **6** takes an *E* configuration. This can be anticipated from the conformation of 2-amino-5-phosphonopentanoate bound to tThrS, which is an analogue for the enamine intermediate (**4**).[4] As W−1 and the ε-amino group of Lys61 exist at the *re* face (Cβ taken as the prochiral center) of **6**, the water-added structure **8** has *R* chirality at Cβ, which is the chirality of L-threonine.

**Transaldimination.** The transaldimination process (**8** → **1**) is comprised of three steps. In the first step, the Lys61 ε-amino group performs a nucleophilic attack on PLP C4′ to form a tetrahedral Lys61−PLP−L-threonine intermediate (geminal diamine: $\mathbf{8}^{\mathbf{1}}$). This reaction can be performed by a 120° rotation of the Cδ−Cε single bond of the Lys61 side chain. The activation barrier for the N−C bond formation was calculated to be 9.2 kcal mol$^{-1}$ ($G(\mathbf{TS}^{8,81}) - G(\mathbf{8})$). The product intermediate $\mathbf{8}^{\mathbf{1}}$ is as stable as **8**.

In the second step, a proton transfer from N of the Lys61 moiety to N of the L-threonine moiety ($\mathbf{8}^{\mathbf{1}} \rightarrow \mathbf{1}^{\mathbf{8}}$) occurs because the protonation at N of the L-threonine moiety is necessary for the elimination of L-threonine. Proton transfer through the phenolate O (O3′) of PLP was found to be the most energetically favorable path. Thus, the step is further divided into two substeps; in the first substep, one proton is transferred from N of the Lys61 moiety to the phenolate O of the PLP moiety, and in the second substep, the proton is transferred from the phenolate O to N of the L-threonine moiety. The transition state ($\mathbf{TS}^{81,18}$) was located at the second substep. The calculated free energy barrier was 11.9 kcal mol$^{-1}$ ($G(\mathbf{TS}^{81,18}) - G(\mathbf{8}^{\mathbf{1}})$).

Salva and co-workers studied the transaldimination reaction via a geminal diamine intermediate using DFT and semi-empirical PM3 methods.[10,11] Their calculated energy barrier at the DFT level was 13.1 kcal mol$^{-1}$ in a model system including one additional water molecule mediating the intramolecular proton transfer.[11] Another calculated energy barrier was 12.6 kcal mol$^{-1}$ for ornithine decarboxylase by Cerqueria et al.[12] It may be considered that W5 in ThrS corresponds to the bridging water in these calculations. However, W5 is strongly hydrogen bonded to Lys116 and Thr85, and is located opposite to the germinal diamine with respect to the PLP plane. Therefore, it is less likely that W5 is involved in the proton transfer. Another possibility is the existence of some water molecules near the PLP, which could mediate the proton transfer. For all the X-ray structures deposited in the Protein Data Bank, however, 15 ThrS structures do not contain such


dx.doi.org/10.1021/ja408780c | J. Am. Chem. Soc. 2014, 136, 4525−4533

water molecules except for W5. Our calculations could provide a similar and even lower energy barrier (11.9 kcal mol$^{-1}$) without assuming a water molecule bridging the two N atoms in the geminal diamine.

Following the first two steps, there is the last step which involves the elimination of L-threonine from $\mathbf{1}^{8}$ to form the internal aldimine ($\mathbf{1}^{Thr}$). In our calculation, however, this step was not observed. This will be discussed later in this paper.

The side reaction of the $\alpha$-aminocrotonate formation ($\mathbf{6} \rightarrow \mathbf{1}^{AC}$) is essentially similar to the main reaction of the L-threonine formation ($\mathbf{8} \rightarrow \mathbf{1}^{Thr}$); the reaction proceeds in three steps, in which a geminal diamine intermediate is first formed ($\mathbf{6}^{1}$), and then the proton is transferred from N of the Lys61 moiety via the phenolate O of PLP to N of the $\alpha$-aminocrotonate moiety to form the second geminal diamine ($\mathbf{1}^{6}$), and finally, $\alpha$-aminocrotonate is eliminated ($\mathbf{1}^{AC}$). The transition state was also found in the proton transfer from the phenolate O to N of the $\alpha$-aminocrotonate moiety. Despite these similarities, the transition energy of $\mathbf{TS}^{61,16}$ is higher than $\mathbf{TS}^{81,18}$ by 3.9 kcal mol$^{-1}$. This difference in the transition energy may be interpreted as follows. During the $\alpha$-aminocrotonate formation, the C$\alpha$−N bond of the $\alpha$-aminocrotonate moiety rotates and breaks the conjugation of the lone pair electrons of N to the C$\alpha$−C$\beta$ double bond, resulting in destabilization of the transition states. On the other hand, for the L-threonine formation, the threonine hydroxy group forms a hydrogen bond with the phosphate ion and this hydrogen bond assists in the approach of the threonine N to the phenolate O of PLP in $\mathbf{TS}^{81,18}$ (Figure 4). These differences may contribute to the higher reaction barrier of $\mathbf{TS}^{61,16}$ compared to $\mathbf{TS}^{81,18}$. It should be noted, however, that we should be careful in comparing the energy levels of $\mathbf{TS}^{61,16}$ and $\mathbf{TS}^{81,18}$. The relative energy levels of **6** and $\mathbf{6}^{H_2O}$, which are required to compare the two transition states, $\mathbf{TS}^{61,16}$ and $\mathbf{TS}^{81,18}$, are difficult to estimate, because the numbers of QM or MM atoms in **6** and $\mathbf{6}^{H_2O}$ are different. For a more reasonable comparison of the two transition states, the $\alpha$-aminocrotonate formation reaction with one additional water (W−1) was investigated ($\mathbf{6}^{H_2O} \rightarrow \mathbf{1}^{AC,H_2O}$). The relative energies of $\mathbf{TS}^{6,61,H_2O}$, $\mathbf{6}^{1,H_2O}$, $\mathbf{TS}^{61,16,H_2O}$, and $\mathbf{1}^{AC,H_2O}$ compared to $\mathbf{6}^{H_2O}$ were calculated to be 8.1, 7.1, 34.5, and 17.0 kcal mol$^{-1}$, which are 1.8, 5.2, 12.4, and 10.4 kcal mol$^{-1}$, respectively, higher than the corresponding value of the pathway $\mathbf{6} \rightarrow \mathbf{1}^{AC}$. This indicates that $\mathbf{6}^{H_2O}$ is stabilized compared to the other states ($\mathbf{TS}^{61,16,H_2O}$, $\mathbf{1}^{AC,H_2O}$). From the optimized structure of $\mathbf{6}^{H_2O}$, there is a short hydrogen bond between the water (W−1) and Lys61 residue, but the hydrogen bond is weakened in $\mathbf{6}^{1,H_2O}$ and missing in other states, explaining the change in the relative energy. Thus, even if we assume that the side reaction starts from $\mathbf{6}^{H_2O}$ instead of **6**, we can conclude that $\mathbf{TS}^{61,16,H_2O}$ has a higher energy level than $\mathbf{TS}^{81,18}$, and can explain the reaction specificity of tThrS to produce L-threonine. However, this does not rule out the possibility that the side reaction starts from **6**. A more detailed study of the relative energy levels of **6** and $\mathbf{6}^{H_2O}$ is required to compare the transition states of the main and side reactions.

**UV/vis Spectra.** The UV/vis spectra were evaluated for all the intermediate states (shown in Figure 5). The calculated absorption peaks were 400, 423, and 360 nm for **6**, **7**, and **8**, respectively, which correspond to the experimental values of 450, 476, and 416 nm. Although the calculated excitation energies are all blue-shifted by approximately 50 nm, the characteristic features of the UV/vis spectra, such as the largest absorption of the quinonoid (**7**) on the long-wavelength side,

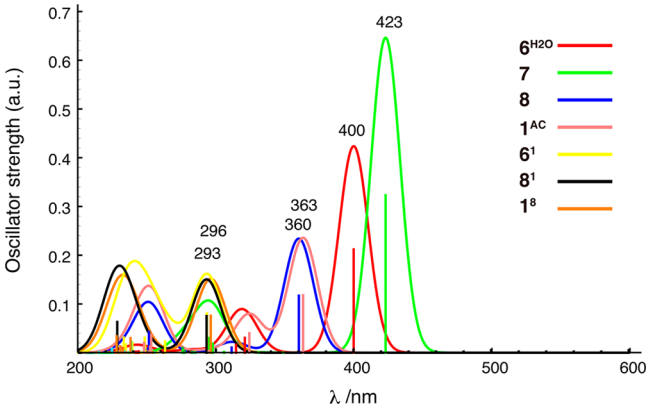


**Figure 5.** Calculated UV/vis spectra of key intermediate states. The absorption bands are calculated using the Gaussian model with a half-bandwidth of 25 nm.

are properly reproduced. These excitations are all assigned to the $\pi$−$\pi^*$ transitions. The quinonoid intermediate (**7**) has highly delocalized frontier molecular orbitals (Figure S5, Supporting Information).

State **6** exists as both ketoenamine and enolimine isomers. The enolimine isomer ($\mathbf{6}^{en}$) is calculated to be slightly higher in energy by 3.5 kcal mol$^{-1}$ and shows a broad UV/vis spectrum with peaks at 325 and 270 nm (the optimized structure of $\mathbf{6}^{en}$ and the UV/vis spectrum are shown in Figures S4.6 and S6, respectively, Supporting Information). Experimentally, a small absorption at around 330 nm is observed in the spectra of **6**, which can be attributed to the enolimine form ($\mathbf{6}^{en}$). It can be clearly seen that the spectra of **8** and $\mathbf{1}^{AC}$ are very similar with absorption band maxima at 360 nm. The spectra of the geminal diamines of $\mathbf{8}^{1}$, $\mathbf{1}^{8}$, and $\mathbf{6}^{1}$ are more blue-shifted with absorption maxima of around 300 nm. The absorptions of these geminal diamines correspond to the experimental values of 343 nm in serine hydroxymethyltransferase[13] and 345 nm in the H188K mutant GDP-4-keto-6-deoxy-D-mannose 3-dehydratase.[14] The consistency of the calculated spectra with the obtained spectra of the intermediates supports the validity of the assignment of the intermediates detected in the stopped-flow experiments.[5]

**Protonation States.** The p$K_a$ of the PLP N1 of the PLP−methylamine aldimine is 5.8 in water,[15] and thus, PLP N1 is unprotonated under normal conditions. For most PLP enzymes other than the fold type II enzymes, the PLP N1 is protonated by forming a salt bridge with a carboxylate group of Asp or Glu.[4,16−18] The protonation at N1 increases the electron-withdrawing ability of the PLP ring. In alanine racemase, a fold type III enzyme, the PLP N1 is unprotonated and is a hydrogen bond acceptor from Arg219.[19] Toney and co-workers revealed that the N1-unprotonated PLP provides a feasible reactivity in alanine racemase,[20,21] which was later supported by the QM/MM calculations by Major and Gao.[22] The unprotonated PLP N1 is also expected for the fold type II enzymes, such as *O*-acetylserine sulfhydrylase and serine dehydratase, where the Ser and Cys residues form a hydrogen bond with the PLP N1.[23−25] ThrS also belong to the fold type II, and in our QM/MM calculation, the PLP N1 is unprotonated and acts as a hydrogen bond acceptor for Thr317. If the PLP N1 is protonated, state **7** is too stabilized by 18 kcal mol$^{-1}$ and the activation barrier of $\mathbf{TS}^{6,7}$ vanishes in the reaction of $\mathbf{6} \rightarrow \mathbf{7}$ (Figure S7, Supporting Information). This energy profile is completely inconsistent with the experimental free energy profile, and the results support the unprotonated pyridine N.


dx.doi.org/10.1021/ja408780c | J. Am. Chem. Soc. 2014, 136, 4525−4533

The protonation state of the phosphate ion is another important issue in the reaction mechanism. As the $pK_{a2}$ of the phosphate ion is 7.2, both the $HPO_4^{2-}$ and $H_2PO_4^-$ forms can be populated under normal conditions. In the $H_2PO_4^-$ form, a hydrogen atom is shared by the phosphate ion and the Lys61 $\varepsilon$-amino group, and state **7**, where the $\varepsilon$-amino group accepts a proton from the attacking water molecule, is considerably destabilized by 9.9 kcal mol$^{-1}$ relative to **6** (Figure S7, Supporting Information). Thus, $HPO_4^{2-}$ is the reactive form in the L-threonine formation pathway.

**Other Reaction Pathways.** Energy profiles for the possible reaction pathways other than the pathway described above (path 1) were calculated (Figure S8, Supporting Information). In path 3, the phosphate ion acts as a general base in the **6** → **7** reaction, a proton is transferred from the phosphate ion to the Lys61 $\varepsilon$-amino group, and the protonated $\varepsilon$-amino group of Lys61 acts as a general acid in the **7** → **8** reaction. In path 2, the 5′-phosphate group of PLP acts as a general base in the **6** → **7** reaction, and a direct proton transfer from the hydroxy group to C$\alpha$ occurs in the **7** → **8** reaction, followed by a transfer of a proton from the 5′-phosphate group of PLP to the hydroxy group. In addition, with respect to the proton transfer ($\mathbf{8}^{\mathbf{1}}$ → $\mathbf{1}^{\mathbf{8}}$) during the transaldimination process, a direct proton transfer can be considered. The energy profiles are summarized in Figure S9 (Supporting Information).

For path 3, the calculated activation barrier of the **6** → **7** reaction is ∼30 kcal mol$^{-1}$. The high energy barrier is attributed to the long distance between the attacking water molecule (W−1) and the phosphate ion. Path 3 also has a high energy barrier (≫17 kcal mol$^{-1}$) at the step **7** → **8**.

For path 2, the generated monoprotonated phosphate ester state in **7** ($\mathbf{7}^{\mathbf{MP}}$) is stable compared to the protonated $\varepsilon$-amino group state of Lys61 in **7**. The state $\mathbf{7}^{\mathbf{MP}}$ can be converted to **7** with a low activation barrier of 3.2 kcal mol$^{-1}$. However, the direct proton transfer pathway for the step **7** → **8** along path 2 has a high energy barrier of ∼45 kcal mol$^{-1}$. This is considered to have arisen from the unstable four-membered transition state structure. Therefore, in the **6** → **7** reaction, both path 1 (**6** → **7**) and path 2 (**6** → $\mathbf{7}^{\mathbf{MP}}$ → **7**) are possible, while only path 1 is possible in the **7** → **8** reaction. The proton abstraction of the reacting water by the phosphate group of PLP can operate in the water-addition reaction only if the proton is again transferred to the $\varepsilon$-amine group of Lys61 and merges into path 1 in the **7** → **8** reaction.

The direct proton transfer ($\mathbf{8}^{\mathbf{1}}$ → $\mathbf{1}^{\mathbf{8}}$) of the transaldimination process (path $2^{81,18}$), in which the proton does not pass through the phenol oxygen atom as in path $1^{81,18}$, has a calculated energy barrier of 30 kcal mol$^{-1}$, and this is unlikely to occur. The high energy barrier can be attributed to the rather long N−N distance of 2.4 Å. Also, in path $2^{81,18}$, nitrogen inversions of the amines, which must simultaneously occur upon the proton transfer, are considered to contribute to the high energy barrier. Therefore, the mechanism described in the previous sections (path $1^{81,18}$) is the only possible pathway in the transaldimination process.

**Replenishment of the Reacting Water Molecule.** The proximity of W−1 and W0 suggests that W−1 is supplied by the migration of W0 in $\mathbf{6}^{\mathbf{H_2O}}$. If W0 is not replenished from the solvent, W0 is missing after **7**, and **8** is relatively stabilized by 16.5 kcal mol$^{-1}$ and the reaction will be terminated at **8**. W0 forms a stable hydrogen bond to the phosphate ion and is separated from the bulk solvent only by hydrophilic residues, such as Asn188, Ser155, and Ser248. Therefore, it is expected that a bulk water molecule could easily enter into the W0 position.

**Open−Closed Conformational Change.** Large conformational changes are known by the binding of the substrate to the PLP enzymes, such as aspartate aminotransferase as well as ThrS. In tThrS, the open−closed conformational change is caused by the rotation of the small domain composed of four parallel $\beta$-sheets and surrounding three $\alpha$-helices by about 25° toward the large domain.[4,7,26] The PLP-binding Lys61 does not interact with the small domain, and the motion of Lys61 does not directly induce the overall conformational change. The substrate PLP and the phosphate ion are hydrogen bonded to the active site residues and water molecules. Most of these active site residues come from the large domain. Small domain residues involved in these interactions are Ser84, Thr85, and Asn87. Our calculations show that these residues form tight hydrogen-bond interactions with the phosphate ion, the carboxyl group of the substrate, and O3′ of PLP. All of these residues can contribute to the large conformational change affected by the substrate binding. Because the Ser84 side chain maintains a direct hydrogen bond to the carboxylate group of the product L-threonine, we expect that Ser84 strongly affects the product formation by its mobility. In fact, Ser84 is located in the asparagine loop composed of three residues, Ser84−Thr85−Gly86. The loop region is found in other PLP dependent enzymes, such as *O*-acetylserine sulfhydrylase and serine racemase,[27−29] and is considered to bind to the substrate carboxylate group of the PLP−substrate aldimine. The motion of Ser84 and the loop may induce the large conformation change, which is important for the catalytic specificity.

In our model, L-threonine is not completely dissociated from the geminal diamine $\mathbf{1}^{\mathbf{8}}$, with the Mulliken bond order for C4′:PLP−N:PLP being 0.71 (N:PLP indicates the N atom of the substrate/product moiety forming a covalent bond with C4′ of PLO). Thus, the Michaelis complex of the internal aldimine and L-threonine ($\mathbf{1}^{\mathbf{Thr}}$) was not obtained. The Michaelis complex of the internal aldimine and $\alpha$-aminocrotonate ($\mathbf{1}^{\mathbf{AC}}$) was obtained. However, as the Mulliken bond order for C4′:PLP−N:PLP is 0.14, it does not seem to be fully stabilized, because the experimentally estimated energy level of the Michaelis complex is 1.3 kcal mol$^{-1}$ higher than **6**.[5] These results suggest that a large conformational change may take place simultaneously or after the transaldimination to stabilize the Michaelis complex, which could not be reproduced by our current QM/MM calculations.

**The Role of the Phosphate Ion.** The present results showed that the $\varepsilon$-amino group of Lys61 acting as the base catalyst is the energetically more probable model. Despite this, the experimental results showed that the phosphate ion is absolutely required for the reaction flux from **6** to be directed toward the normal reaction pathway.[5] In the normal reaction pathway, the phosphate ion forms a hydrogen bond with the O atom of the attacking water molecule (W−1) in $\mathbf{6}^{\mathbf{H_2O}}$, and this hydrogen bond is maintained until $\mathbf{1}^{\mathbf{8}}$ (the O atom of W−1 becomes the hydroxy O of the L-threonine moiety). On the other hand, this hydrogen bond is missing in the side reaction pathway. Therefore, the interaction of the phosphate ion with the product moiety, as revealed in this study, is considered to have important roles in lowering the energy levels of the transition states in the normal reaction pathway as compared to those of the side reaction pathway. We interpret the role of the phosphate ion as follows. In the transition state ($\mathbf{TS}^{\mathbf{81,18}}$) of the transaldimination to form L-threonine, the proton is between


dx.doi.org/10.1021/ja408780c | J. Am. Chem. Soc. 2014, 136, 4525−4533

the PLP O3′ atom and the N atom of the L-threonine moiety. Therefore, the O3′ atom, which resides in the plane containing the PLP pyridine ring, approaches the L-threonine N at the transition state, and this movement is assisted by the hydrogen bond between the phosphate ion and the $\beta$-hydroxy O, which pulls the L-threonine moiety toward the plane containing the PLP pyridine ring. As this hydrogen bond is missing in the transaldimination reaction to form $\alpha$-aminocrotonate, its transition state, which similarly locates at the second substep (proton transfer from O3′ to the N of the $\alpha$-aminocrotonate), is less stabilized as compared to the transaldimination to form L-threonine. The transition state of protonation at C$\alpha$ (**TS**$^{7,8}$) is brought about by the approach of C$\alpha$ to the $\varepsilon$-amino group of Lys61. Therefore, the hydrogen bond between the phosphate ion and the $\beta$-hydroxy group may also lower the energy level of **TS**$^{7,8}$.

From the observation that the less basic sulfate ion cannot substitute phosphate ion, we considered that the phosphate ion acts as a base catalyst for the addition of water to **6**.[5] However, the present study shows that another interpretation is more plausible. As sulfuric acid is a strong acid with p$K_{a2}$ = 1.92, the sulfate ion is not protonated over a wide range of pH, and therefore cannot be a hydrogen bond donor. The strong acid nature of sulfuric acid also indicates that the sulfate ion is a weak hydrogen bond acceptor. As a result, the hydrogen bond that stabilizes **TS**$^{81,18}$ and **TS**$^{7,8}$ in the presence of the phosphate ion is less likely to be formed, and this can be the reason for the increased energy levels of the transition states of the normal reaction pathway in the presence of the sulfate ion. The detailed QM/MM study on the reaction in the presence of the sulfate ion would examine this proposal. Furthermore, similar calculation in the absence of either phosphate or sulfate ion would provide information on the structural role of these ions in the catalysis. These studies are now under way in our laboratories.

## CONCLUSION

There were many ambiguities about the protonation states, hydrogen bonds, proton transfer routes, as well as acid/base catalytic groups. Comparative QM/MM calculations with an exhaustive search for the lowest-energy-barrier reaction pathways were performed on the reaction from the PLP−$\alpha$-aminocrotonate aldimine intermediate (**6**), both for the direction of the normal catalytic reaction producing L-threonine and the side reaction yielding $\alpha$-aminocrotonate. Satisfactory agreements with the experimental results were obtained for the free energy profile and the UV/vis spectra in the case of the unprotonated PLP N1 and the monoprotonated phosphate ion. Contrary to the earlier proposal, the phosphate ion is less likely the base for abstracting a proton from the attacking water molecule. Rather, the $\varepsilon$-amino group of Lys61 deprotonates the water and, in turn, donates a proton to C$\alpha$ of the quinonoid intermediate (**7**) to form the PLP−L-threonine aldimine intermediate (**8**). However, the phosphate ion maintains a hydrogen bond with the $\beta$-hydroxy group of the L-threonine moiety following the nucleophilic attack of the water molecule on C$\beta$ of **6**. The absence of this hydrogen bond may account for the higher energy barrier of the side reaction releasing $\alpha$-aminocrotonate. The QM/MM calculations presented here have allowed us to clarify the proton transfer events in the normal and side reaction pathways and the energetic preference for the normal reaction pathway. Additionally, a new mechanism, in which a proton temporarily resides at the phenolate O3′ of PLP, was proposed for the transaldimination process. As this process is common to all the PLP enzymes, this finding is of great importance for generally discussing the catalytic mechanism of PLP enzymes.

## ASSOCIATED CONTENT

### Supporting Information

Full reaction mechanism, QM/MM system, full energy profile, enlarged views of all the optimized structures, important frontier orbitals, UV/vis spectra, reaction energy profiles for other states, illustration of other reaction pathways, schematic energy profile for other reaction pathways, details of free energies, relative energies at higher theoretical levels, bond orders, charge population analyses, UV/vis absorption wavelengths, and *xyz* coordinates for all of the optimized states. This material is available free of charge via the Internet at http://pubs.acs.org.

## AUTHOR INFORMATION

### Corresponding Author

mshoji@ccs.tsukuba.ac.jp

### Notes

The authors declare no competing financial interest.

## ACKNOWLEDGMENTS

This research was supported by (1) "Interdisciplinary Computational Science Program" at the Center for Computational Sciences, University of Tsukuba, Japan; (2) the HA-PACS Project for advanced interdisciplinary computational sciences by exa-scale computing technology; (3) "Joint Usage/Research Center for Interdisciplinary Large-scale Information Infrastructures" at Information Technology Center, The University of Tokyo, Japan; and (4) the Supercomputer Center, Institute for Solid State Physics, University of Tokyo, Japan. This research was supported by a Grant-in-Aid for Young Scientists (B; No. 24750007) from the Japan Society for the Promotion of Science.

## REFERENCES

(1) Laber, B.; Gerbling, K. P.; Harde, C.; Neff, K. H.; Nordhoff, E.; Pohlenz, H. D. *Biochemistry* **1994**, *33*, 3413−3423.
(2) Hayashi, H. *J. Biochem.* **1995**, *118*, 463−473.
(3) Franco, M. G.; Ehlert, S.; Messerschmidt, A.; Marinkovic, S.; Huber, R.; Laber, B.; Bourenkov, G. P.; Clausen, T. *J. Biol. Chem.* **2002**, *277*, 12396−12405.
(4) Omi, R.; Goto, M.; Miyahara, I.; Mizuguchi, H.; Hayashi, H.; Kagamiyama, H.; Hirotsu, K. *J. Biol. Chem.* **2003**, *278*, 46035−46045.
(5) Murakawa, T.; Machida, Y.; Hayashi, H. *J. Biol. Chem.* **2011**, *286*, 2774−2784.
(6) Fromme, J. C.; Bruner, S. D.; Yang, W.; Karplus, M.; Verdine, G. L. *Nat. Struct. Biol.* **2003**, *10*, 204−211.
(7) Valiev, M.; Bylaska, E. J.; Govind, N.; Kowalski, K.; Straatsma, T. P.; van Dam, H. J. J.; Wang, D.; Nieplocha, J.; Apra, E.; Windus, T. L.; de Jong, W. A. *Comput. Phys. Commun.* **2010**, *181*, 1477−1489.
(8) Yanai, T.; Tew, D. P.; Handy, N. C. *Chem. Phys. Lett.* **2004**, *393*, 51−57.
(9) Grimme, S.; Antony, J.; Ehrlich, S.; Krieg, H. *J. Chem. Phys.* **2010**, *132*, 154104−19.
(10) Salva, A.; Donoso, J.; Frau, J.; Munoz, F. *J. Phys. Chem. A* **2004**, *108*, 11709−11714.
(11) Salva, A.; Donoso, J.; Frau, J.; Munoz, R. *Int. J. Quantum Chem.* **2002**, *89*, 48−56.
(12) Cerqueira, N. M. F. S. A.; Fernandes, P. A.; Ramos, M. J. *J. Chem. Theory Comput.* **2011**, *7*, 1356−1367.

(13) Rao, J. V. K.; Prakash, V.; Rao, N. A.; Savithri, H. S. *Eur. J. Biochem.* **2000**, *267*, 5967−5976.
(14) Cook, P. D.; Holden, H. M. *Biochemistry* **2007**, *46*, 14215−14224.
(15) Sharif, S.; Huot, M. C.; Tolstoy, P. M.; Toney, M. D.; Jonsson, K. H. M.; Limbach, H.-H. *J. Phys. Chem. B* **2007**, *111*, 3869−3876.
(16) Parsot, C. *EMBO J.* **1986**, *5*, 3013−3019.
(17) Sharif, S.; Fogle, E.; Toney, M. D.; Denisov, G. S.; Shenderovich, I. G.; Buntkowsky, G.; Tolstoy, P. M.; Huot, M. C.; Limbach, H.-H. *J. Am. Chem. Soc.* **2007**, *129*, 9558−9559.
(18) Isupov, M. N.; Antson, A. A.; Dodson, E. J.; Dodson, G. G.; Dementieva, I. S.; Zakomirdina, L. N.; Harutyunyan, E. H. *J. Mol. Biol.* **1998**, *276*, 603−623.
(19) Morollo, A. A.; Petsko, G. A.; Ringe, D. *Biochemistry* **1999**, *38*, 3293−3301.
(20) Spies, M. A.; Toney, M. D. *Biochemistry* **2003**, *42*, 5099−5107.
(21) Spies, M. A.; Woodward, J. J.; Watnik, M. R.; Toney, M. D. *J. Am. Chem. Soc.* **2004**, *126*, 7464−7475.
(22) Major, D. T.; Gao, J. *J. Am. Chem. Soc.* **2006**, *128*, 16345−16357.
(23) Rabeh, W. M.; Cook, P. F. *J. Biol. Chem.* **2004**, *279*, 26803−26806.
(24) Tai, C. H.; Cook, P. F. *Acc. Chem. Res.* **2001**, *34*, 49−59.
(25) Yamada, T.; Komoto, J.; Takata, Y.; Ogawa, H.; Pilot, H. C.; Takusagawa, F. *Biochemistry* **2003**, *42*, 12854−12865.
(26) Droux, C. M.; Biou, V.; Dumas, R. *J. Biol. Chem.* **2006**, *281*, 5188−5196.
(27) Rabeh, W. M.; Cook, P. F. *J. Biol. Chem.* **2004**, *279*, 26803−26806.
(28) Burkhard, P.; Rao, G. S. J.; Hohenester, E.; Schnackerz, K. D.; Cook, P. F.; Jansonius, J. N. *J. Mol. Biol.* **1998**, *283*, 121−133.
(29) Goto, M.; Yamaguchi, T.; Kamiya, N.; Miyahara, I.; Toshimura, T.; Mihara, H.; Kurihara, T.; Hirotsu, K.; Esaki, N. *J. Biol. Chem.* **2009**, *284*, 25944−25952.